

# INDUCTION OF ARTHRITIS IN MICE AND RATS BY POTASSIUM PEROXOCHROMATE AND ASSESSMENT OF DISEASE ACTIVITY BY WHOLE BLOOD CHEMILUMINESCENCE AND <sup>99m</sup>PERTECHNETATE-IMAGING

\*RALF MIESEL, \*HANS KRÖGER, §MACIEJ KURPISZ and  
#ULRICH WESER

*\*Deutsches RheumaForschungsZentrum (German Rheumatology Research Center),  
Department of Biochemistry, Nordufer 20, 13353 Berlin, Germany, Tel.  
++49-30-4542060 Fax ++49-30-4542090; §Institute of Human Genetics, Polish  
Academy of Sciences, Poznan, Poland; #Physiologisch-Chemisches Institut,  
University of Tuebingen, Department of Inorganic Biochemistry, Tübingen, Germany*

*(Received October 13th, 1994; in revised form, November 24th, 1994)*

Arthritis develops in DBA/1xB10A(4R) mice and Wistar rats upon intraplantar injection of potassium peroxochromate ( $K_3CrO_8$ ), and is here quantified by whole blood chemiluminescence (CL) and <sup>99m</sup>perchnetate-imaging (<sup>99m</sup>TcO<sub>4</sub><sup>-</sup>), and related to overt disease symptoms (the arthritis index). During the aqueous decay of  $K_3CrO_8$  to chromate (VI), the chromium(V)-bound oxygen is released as superoxide, hydroxyl radicals, singlet oxygen and hydrogen peroxide, the same reactants, which are produced by activated phagocytes during inflammation. Reactive oxygen species (ROS) trigger the breakdown of the sulfhydryl-dependent antioxidant defence system and induce the nuclear factor kappa B-dependent expression of pro-inflammatory cytokines, which prime phagocytic NADPH oxidases to the enhanced production of ROS. During both the acute inflammatory response and the onset of the secondary response in non-injected paws, the phorbol ester-stimulated ROS production of phagocytes was significantly enhanced ( $p < 0.001$ ) and correlated well to the arthritis index ( $r = 0.797$ ) and the uptake of <sup>99m</sup>TcO<sub>4</sub><sup>-</sup> into inflamed joints. Chromate(VI), formed during the decay of  $K_3CrO_8$ , contributes to the progression of arthritis by inhibition of glutathione reductase, thereby increasing intracellular H<sub>2</sub>O<sub>2</sub> concentrations. In addition, Cr(VI) reduced to Cr(V) by ascorbate, catalyzes hydroxyl radical production in the presence of hydrogen peroxide. A stable loop forms, in which ROS, continuously produced by Cr(VI)/Cr(V) redox-cycling, drive the primary response into chronic self-perpetuating inflammation. We see the main application of  $K_3CrO_8$ -induced arthritis and its assessment by both <sup>99m</sup>TcO<sub>4</sub><sup>-</sup> imaging and chemiluminescent immunosensing of phagocytic activity in unseparated blood as for the rapid screening of novel anti-rheumatic drugs and treatments.

**KEY WORDS:** Chromium toxicity, arthritis, chemiluminescence, reactive oxygen species, Technetium.

## INTRODUCTION

Rheumatic diseases are a major problem in aging societies. It is estimated that the costs of health care for persons with rheumatic diseases and of their lost time from work will approach 1% of the gross national product of USA by the year 2000.<sup>1</sup>

Experimental research on arthritis is hampered by clearly defined animal models. Quite often, the molecular mechanisms of disease etiology are obscured and do not

<sup>1</sup>For Correspondence

allow precise conclusions on the mode of action of potential anti-rheumatic drugs tested in those models. Thus, one of the most valuable models of arthritis, collagen type II induced arthritis (CIA) in mice and rats, suffers from poorly defined cause-effect analyses.<sup>2</sup> CIA can only be induced in animals bearing one of two independent haplotypes, H-2<sup>a</sup> and H-2<sup>r</sup>.<sup>3</sup> This restricted genetic susceptibility is favorable for studies on the genetics of resistance to the disease, but the unpredictable incidence of developing arthritis, which varies from 40–95%, makes the assessment of anti-rheumatic drugs virtually impossible in this model.<sup>4</sup> In addition, conclusions on the importance of cellular and humoral immunity towards the incidence and severity of disease (CIA can be passively transferred with serum concentrate or lymphocytes from arthritic donors into irradiated mice of the same strain) are obscured by the fact that anti-collagen(II) antibodies are found equally distributed in CII-immunized and non-immunized mice and correlate only poorly to the disease activity.<sup>4</sup> It is also reported that the cellular and humoral reactivity to collagen in human patients suffering from rheumatoid arthritis is not specific for a particular type of collagen.<sup>5</sup> In addition, depletion of complement with cobra venom in rats prevents the onset of disease, while not changing the IgG titer to type II collagen.<sup>6</sup> These findings suggest strongly that CIA is in part mediated by immunocomplexes.

Immunocomplexes bind avidly to Fc receptors on phagocytes and induce the oxidative burst-dependent generation of reactive oxygen species by the membrane-bound enzyme NADPH oxidase.<sup>7</sup> Recently, we were able to show the 10fold enhanced phagocytic release of ROS in patients suffering from various rheumatic diseases. Elevated levels of ROS in those patients caused the partial collapse of the sulfhydryl-dependent antioxidant and antioxidant defence system.<sup>8,9</sup> The NADPH oxidase-dependent, acquired dysfunction of phagocytes in rheumatic patients correlated well to the plasmatic levels of tumor necrosis factor alpha (TNF- $\alpha$ ). TNF- $\alpha$  primes NADPH oxidase *via* the accelerated translocation of cytosolic oxidase subunits to the membrane and induces genes coding for the enzyme. The phagocytic hyperreactivity seen in rheumatic patients was also confirmed in experimental models of arthritis and the application of micromolar concentrations of selective inhibitors of NADPH oxidase or low molecular weight antioxidants Cu(PuPy)<sub>2</sub>, an active center analogue of Cu<sub>2</sub>Zn<sub>2</sub>superoxide dismutase) abrogated the onset and progression of disease.<sup>10,11</sup> The acquired imbalance in pro- and antioxidant levels plays a crucial role in maintaining the underlying chronic inflammatory process in rheumatic diseases. A stable loop may form, in which activated phagocytes release oxygen radicals, and these go on to further stimulate lymphocytes, eventually driving the disease into auto-immunization. The dependence on the continuing inflammatory process and its effective modulation by antioxidants and antioxidantases prompted us to develop a simple, overlookable model of chronic inflammation. The aqueous decay of the inorganic compound potassium peroxochromate to superoxide, hydroxyl radicals, singlet oxygen and hydrogen peroxide seemed most appropriate for this purpose as the molecular modes of action of its reactants are clearly defined and reflect sufficiently the *in vivo* oxidative activity of phagocytes during inflammation.<sup>12,13</sup> In addition, the present study reports the use of whole blood chemiluminescence and <sup>99m</sup>TcO<sub>4</sub><sup>-</sup>-imaging for the assessment of disease activity.<sup>10,14</sup>

## MATERIAL AND METHODS

### *Animals and housing*

Both male DBA/1xB10A(4R) mice, weighing 25–30 g, and Wistar rats, weighing 220–250 g, were kept on a standard laboratory diet *ad libitum*. The animals were housed in groups of ten in wire-topped polycarbonate cages with a layer of sawdust as bedding. The cages were located in a room routinely checked for specific pathogen-free (SPF) conditions. The facility had controlled lighting (light: 0700–1900 h), temperature (22°C) and relative humidity (50%).

### *Chemicals*

Unless otherwise indicated all chemicals were purchased from Sigma-Aldrich, Deisenhofen, Germany.

Potassium peroxochromate ( $K_3CrO_8$ ) was synthesized from  $H_2O_2$ ,  $CrO_3$  and KOH following standard procedures, with minor modifications.<sup>15</sup> 100 ml of deionized water was mixed with 100 ml of KOH 25% (w/v) and 25 ml of a 50% solution of  $CrO_3$  in water (w/v). The solution was cooled to  $-4^\circ C$  (ice/salt) and 30 ml of  $H_2O_2$  (30%) added dropwise under vigorous stirring, avoiding the increase of reaction temperature above  $0^\circ C$ . One hour later, the formed crystals are filtered and washed with ice-cold ethanol (90%; v/v), air-dried and kept in an evacuated exsiccator at room temperature. Yield: 50% of  $[H_2O_2]$ .

### *Induction of $K_3CrO_8$ -Arthritis*

$K_3CrO_8$  was dissolved in 0.01 N NaOH. At alkaline pH the aqueous solution of  $K_3CrO_8$  is stable for a minimum of 2 hours, but decays rapidly to superoxide ( $O_2^-$ ), hydroxyl radicals ( $\cdot OH$ ), singlet oxygen ( $^1\Delta gO_2$ ), hydrogen peroxide ( $H_2O_2$ ), and chromate(VI) ( $CrO_4^{2-}$ ) at physiological pH. The  $K_3CrO_8$ /NaOH solution was diluted with an equal volume of phosphate-buffered saline (PBS) pH 7.4 within a syringe and 25  $\mu l$  administered immediately by intraplantar application into the left hindpaws of mice anaesthetized with diethyl ether to a final concentration of 3  $\mu mol/kg$  of  $K_3CrO_8$ . The same volume of solvent (PBS/0.01 N NaOH 1:2) was injected into the paws of control animals. For convenience and easier handling the  $K_3CrO_8$ /0.01 N NaOH solution can be used without prior dilution with PBS. In injected paws, NaOH (0.01 N) causes oedema formation of rather short duration, which does not influence the chronic course of the disease.

### *Determination of Arthritis Index*

The physical symptoms of arthritis were judged by a standard grading system routinely used to assess arthritis:<sup>16</sup>

0 normal paws; 1 erythema of toes; 2 erythema and swelling of paws; 3 swelling of ankles; 4 complete swelling of the whole leg and incapacity to bend it. The maximum achievable score is thus 16.

### *Light Microscopy*

On day 21 after the induction of arthritis the animals were killed by ether anaesthesia. The hind legs were removed in toto and fixed in 8% formaldehyde. After dissection of

both paws and knee joints and decalcification in 5% formic acid, the tissues were processed and embedded in paraffin wax. Sections of 2–3  $\mu\text{m}$  were cut with a Reichert microtome (Reichert, Vienna, Austria) and stained with haematoxylin/eosin.

#### *Assessment of Arthritis by Whole Blood Chemiluminescence (CL)*

Blood was collected from the median tail artery into polystyrene tubes coated with 10 mM EDTA (Greiner, Frickenhausen, Germany) from five animals per group at alternate days. Alternatively, blood was collected in the same way from the retro-orbital blood sinus. The formation of superoxide was determined by chemiluminescence in a Berthold LB 953 (Wildbad, Germany) luminometer in the presence of lucigenin, within two hours of collection, on duplicate samples. Each 1 ml sample contained 100  $\mu\text{l}$  EDTA-anti-coagulated blood, 100  $\mu\text{M}$  lucigenin, 100  $\mu\text{M}$  diethyldithiocarbamate in RPMI 1640 pH 7.4 (Gibco, Paisley, Scotland) without phenol red. The mixture was equilibrated for 10 minutes at 37°C and the reaction started by the automated injection of 0.5  $\mu\text{M}$  12-O-tetradecanoylphorbol-13-acetate (TPA) in deionized water. The resulting chemiluminescence was recorded for 60" at 37°C and integrated.

#### *Induction of $\text{K}_3\text{CrO}_8$ -Arthritis in Rats and its Assessment by $^{99\text{m}}\text{TcO}_4^-$ -Imaging*

Male Wistar rats were anaesthetized with diethyl ether and 3  $\mu\text{mol/kg}$   $\text{K}_3\text{CrO}_8$  administered by intraplantar application into the left hind-paws. Forty-eight hours later and on day 12, the animals were narcotized by ip application of 40 mg/kg pentobarbital-sodium prior to the iv application of 500  $\mu\text{Ci}$   $\text{Na}^{99\text{m}}\text{TcO}_4$  in PBS into the tail vein and the inflammatory response quantified scintigraphically using a Elscint Apex 409 gamma camera (Elsint, Wiesbaden, Germany).<sup>10</sup> Solvent treated animals served as controls. Both arthritis index and whole blood CL were determined as described above.

#### *Statistical Analysis*

All data were analyzed with Friedman's nonparametric test and adjusted by Dunn's multiple comparison test using the *Instat 2.01* statistics program (GraphPad, San Diego, CA) for Apple/Macintosh and are presented as means  $\pm$  standard deviations (SD).  $P < 0.05$  was considered significant. Pearson's correlation coefficient ( $r$ ) was used for the linear correlation of data.

## RESULTS

Groups of DBA/1xB10A(4R) hybrid male mice (which were part of a larger study on the genetics of resistance to arthritis) and male Wistar rats were intraplantarly injected with 3  $\mu\text{mol/kg}$  of  $\text{K}_3\text{CrO}_8$  by the method described above, and were then scored daily for visible signs of arthritis over a period of 3 weeks. Samples of blood were examined for their ability to generate chemiluminescence upon stimulation with TPA. In addition, the  $\text{K}_3\text{CrO}_8$ -induced swelling of paws was monitored by  $^{99\text{m}}\text{TcO}_4^-$ -imaging.

#### *Arthritis Index*

The disease course shown in figure 1 is representative of five other experiments, which gave similar results, with only minor variations of disease severity.

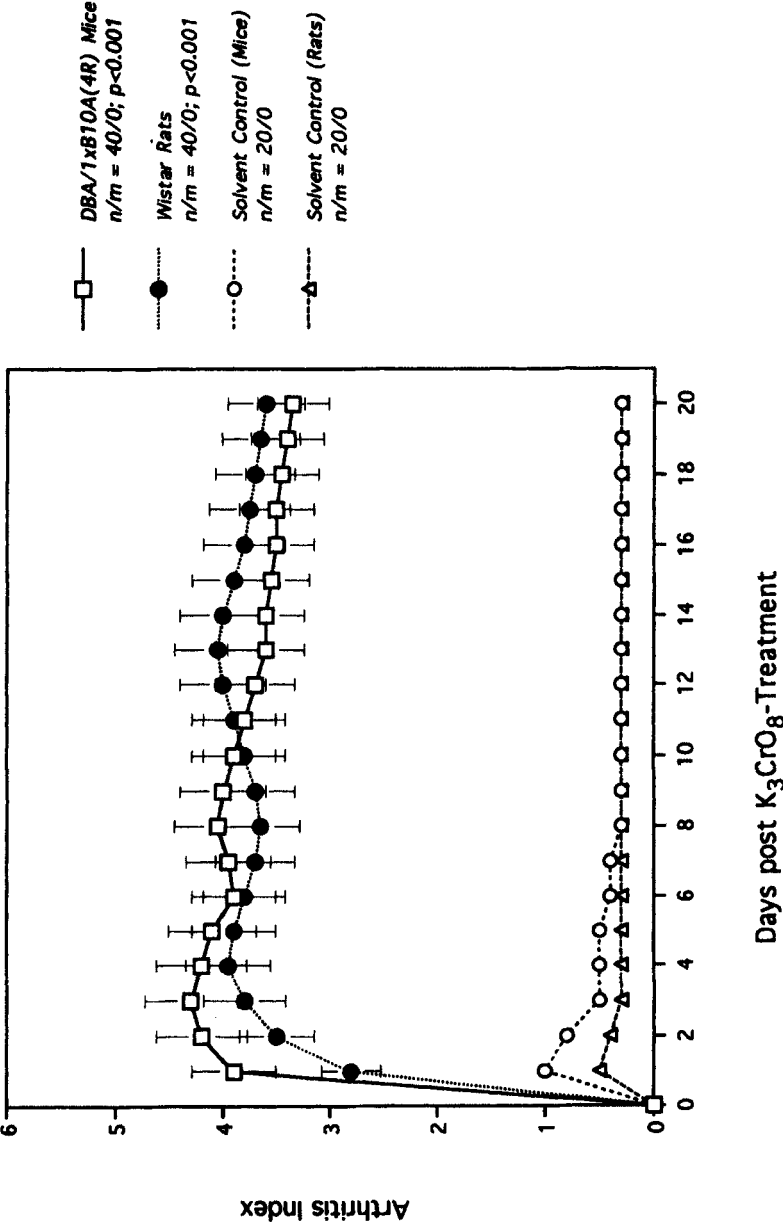


FIGURE 1  $K_3CrO_8$ -induced arthritis in DBA/1xB10A(4R) male mice and Wistar rats. Means and standard deviations of arthritis index, measured daily over a 3-week period; n number of animals; m mortality.

One hundred % of the animals developed an acute inflammation, with an average peak score of about four.

Within 24 hours the inflammatory lesion was massively infiltrated by polymorphonuclear leukocytes followed by the invasion of monocytes after 48 hours. While the oedema formation at the site of injection peaked at days 2–3 in mice and at day 4 in rats and started slowly to decline, a secondary swelling developed in non-injected hindpaws, which peaked at day 8 in mice and at day 13 in rats. The forepaws were usually less involved (slight erythema in some animals). In 40% of  $K_3CrO_8$ -treated animals, ankylosis of the knee joints led to the complete incapacity to bend the leg. Skin lesions and subcutaneous nodules developed in less than 10% of animals and hair loss was observed in approximately 2% of mice. Quite common was the whitening of the tail tip without necrosis, which typically started at day 8. After 14 days the arthritis index began to wane, but stayed at high levels for more than 40 days, though to a somewhat varying degree. While approximately 20% of both rats and mice recovered completely, the remainder showed the typical histopathological picture of synovial hypertrophy, pannus formation, joint subluxation and deformation of articulating surfaces.<sup>17</sup> The original site of injection was filled with fibrin deposits. Section of livers, spleens and hearts did not reveal any morphological alterations. The disease course in mice did not differ significantly, when the parental strains DBA/1 or B10A(4R) were used, although DBA/1 mice showed a slight tendency to develop a more severe secondary swelling in non-injected paws than the B10A(4R) or hybrid DBA/1xB10A(4R) strains (data not shown).

### *Whole Blood CL*

For the chemiluminescence assay, as stated in the methods section, duplicate samples were read within 2 hours of collection, with an integration time over the oxidative burst from 0' to 60". This procedure was established on the basis of the following information. Duplicates differed by <10%. Holding blood on ice for an additional 2 hours reduced the burst by an average of 12%. Lucigenin was chosen for use as amplifier because it reacts exclusively with superoxide and thus more selectively reflects the NADPH oxidase activity than the alternative amplifier luminol.<sup>18</sup> Unlike lucigenin, luminol penetrates readily cell membranes and measures both the intra- and extracellular levels of hydrogen peroxide as well as the myeloperoxidase-associated oxygen radical production and is therefore affected by the activity of the hydrogen peroxide degrading enzymes glutathione peroxidase and catalase.<sup>19</sup> The exclusive reaction of lucigenin with superoxide and the virtual absence of extracellular superoxide dismutases minimizes interference with the assay.<sup>20</sup>

The choice of activators of the oxidative burst is also critical and depends on what one wants to measure. While complement C3b, iC3b and immunoglobulin opsonized zymosan particles from yeast cell walls as well as the chemotactic peptide FLMP rely upon ligation of complement and binding to cell surface receptors to trigger CL *via* both diacylglycerol generation and calcium influx, the non-receptor mediated stimulation by the phorbol ester TPA proceeds through the protein kinase C-dependent phosphorylation of NADPH oxidase subunits.<sup>21</sup> Surface receptors, i.e. Fc receptors on neutrophils, have been shown to be upregulated very quickly during cell separation or even by contact of whole blood to the CL tubes, what may give erratic results. Our lab prefers the use of non-receptor mediated activation by TPA. The detailed molecular mechanisms of TPA-induced assembly of NADPH oxidase to the active enzyme are sufficiently understood.<sup>22</sup>

Thus, 100  $\mu$ l samples of whole, EDTA-stabilized murine blood, were checked for the generation of chemiluminescence upon stimulation with TPA (figure 2).



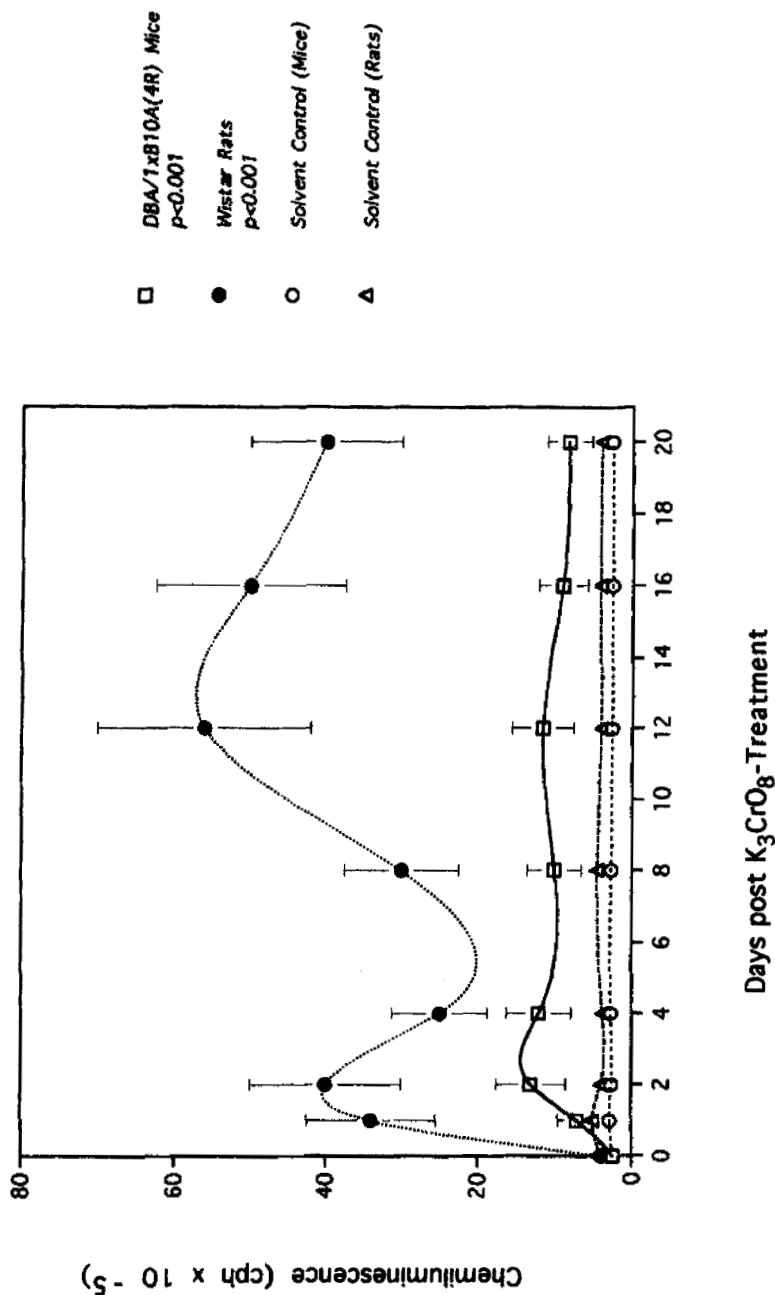


FIGURE 2 Whole blood chemiluminescence and K<sub>3</sub>CrO<sub>8</sub>-induced arthritis: Five animals per group sampled at different time points after the initial induction of arthritis. Means and standard deviations of four independent experiments. The whole blood chemiluminescence of disease groups and solvent controls differ significantly ( $p < 0.001$ ). The experimental details are described in *Materials and Methods*.

When compared to healthy mice, 6fold elevated levels of phagocytic superoxide production were detected in mice suffering from  $K_3CrO_8$ -induced arthritis. The CL measurements of the disease group differed significantly from healthy animals ( $p < 0.001$ ). Leukocytes of both groups were quantified in a coulter counter after lysis of erythrocytes. A slight though insignificant increase in the numbers of leukocytes was monitored in arthritis mice and rats ( $p > 0.05$ ), which had no detectable influence on the CL measurements. The CL curves showed biphasic kinetics. At day 3 the acute inflammatory response peaked with an average of  $1.4 \times 10^6$  counts per hour (cph), which coincided with the swarming of neutrophils and monocytes into the inflamed area. The acute CL response declined then progressively until day 6. A secondary response followed, which peaked on day 12. The CL curve began then to wane slowly. The secondary CL response correlated to the development of arthritis in non-injected paws. The CL curves of healthy animals stayed at low levels of about  $0.2 \times 10^6$  cph and did not vary significantly over the observed period.

Unlike the strong resemblance of arthritis indices in the mouse and rat models described above, the TPA-induced CL responses in  $K_3CrO_8$ -treated Wistar rats differed from those obtained in DBA/1xB10A(4R) mice. In general, the CL responses were 4–5 fold higher than in mice, but the bimodality of CL kinetics remained the same. The primary CL response of rats peaked at day 2 with  $4 \times 10^6$  cph and preceded the manifestations of overt symptoms by 48 hours (figure 1). The secondary response, which peaked at days 12–13 with an average of  $6 \times 10^6$  cph, was markedly enhanced, when compared to that of mice and correlated well to the development of arthritis in non-injected paws.

### *Correlating CL and Arthritis Index*

The arthritis index and whole blood CL of  $K_3CrO_8$ -treated mice correlated positively with an overall correlation coefficient of  $r = 0.863$  (figure 3).

The arthritis index and CL correlated best to the primary acute inflammatory phase (days 1–3) and to the onset of the secondary immunological response (days 7–12).

A correlation coefficient of  $r = 0.797$  was obtained for  $K_3CrO_8$ -treated Wistar rats.

### *$^{99m}Tc$ -Imaging*

Rats suffering from peroxochromate arthritis were narcotized with 40 mg/kg pentobarbital-sodium (ip) prior to the intravenous injection of 500  $\mu$ Ci  $Na^{99m}TcO_4^-$ . The distribution of  $^{99m}TcO_4^-$  was followed by  $\gamma$ -scintigraphy (figures 4a–c).

While  $^{99m}TcO_4^-$  was taken up to a negligible extent into the paws of healthy animals (figure 4a), high activities were monitored in  $K_3CrO_8$ -injected paws after 48 hours (figure 4b). At day 12, when the secondary response is at its height (figures 1 and 2), significant amounts of  $^{99m}TcO_4^-$  were also scanned in non-injected paws (figure 4c), which reflected the development of arthritis in non-injected paws at that time (figure 1) and correlated sufficiently to the increase of CL (figure 2).

## DISCUSSION

The present study reports the induction of arthritis by potassium peroxochromate in male DBA/1xB10A(4R) hybrid mice and Wistar rats and its assessment by both whole blood chemiluminescence and  $^{99m}TcO_4^-$ -imaging. The onset, progression and remission



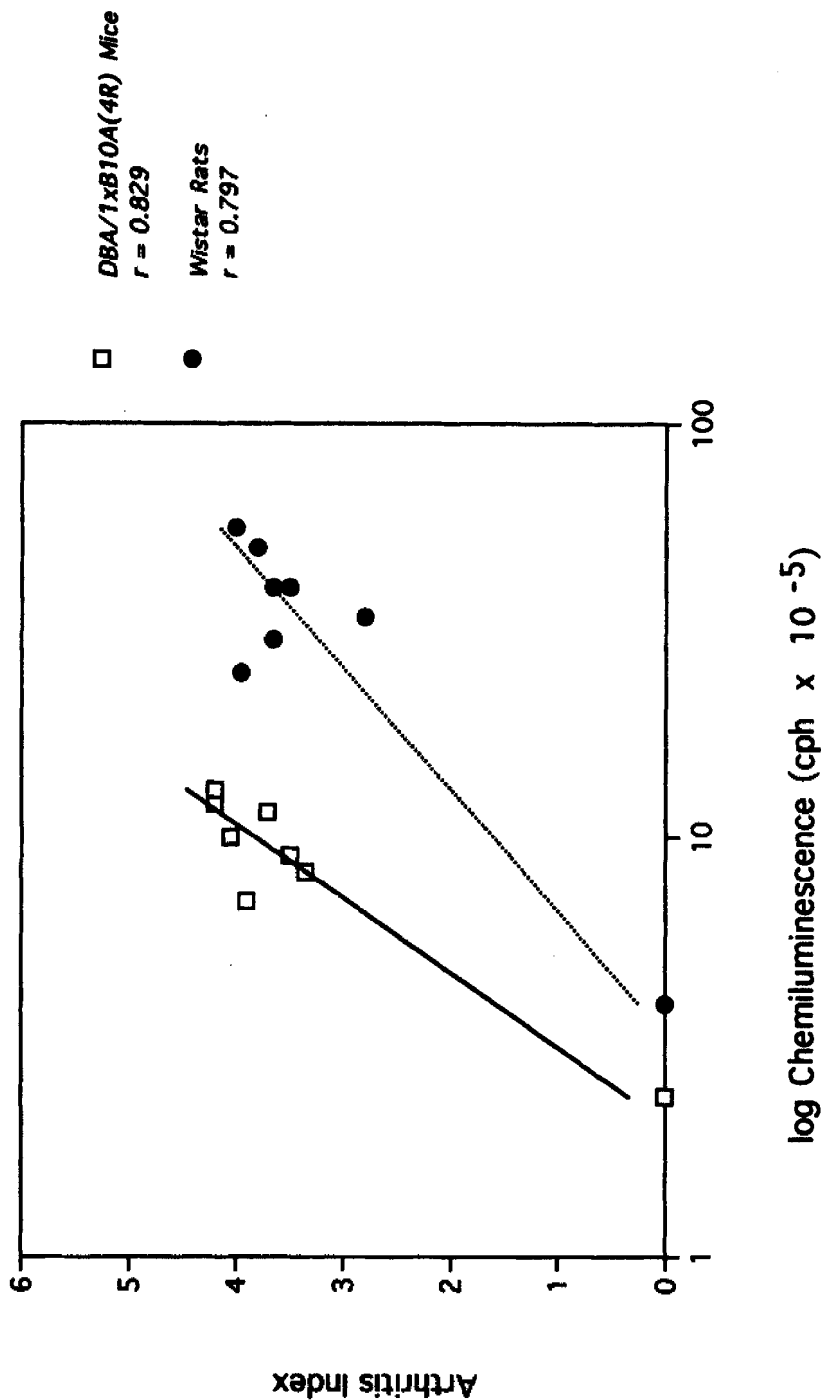


FIGURE 3 Correlation between arthritis index and whole blood chemiluminescence in mice and rats suffering from  $K_2CrO_7$ -arthritis. Pearson's correlation coefficient ( $r$ ) was used for the linear regression.

of arthritis correlated sufficiently to TPA-stimulated phagocytic responses in unseparated blood and to the uptake of  $^{99m}\text{TcO}_4^-$  into inflamed paws. Our findings indicate that chemiluminescence assays of the oxidative burst from granulocytes and monocytes can be used in immunosensing phagocytic hyperreactivity in arthritis in mice and rats. Whole blood CL offers a rapid, convenient, minimal-invasive and quantitative method, which relates well to overt symptoms of arthritis. In addition, it can be applied repeatedly on the same individual and may serve as a surrogate marker for the long-term monitoring of disease activity. The long period observation of arthritis has hitherto been something of a deterrent in most experimental models of arthritis. There is a strong need for rapid quantitative methods for the assessment of disease activity, which could supplement the lengthy process of histological evaluation or the determination of enzyme activities such as myeloperoxidase or N-acetyl- $\beta$ -D-glucosamidase in homogenized paws or amyloid P in serum, which correlate only poorly to the physical symptoms of arthritis.<sup>4</sup> The assay here described offers a promising answer to this need. During inflammation the NADPH oxidase of granulocytes and monocytes becomes primed so as to attain an activated state, which upon a second stimulus (e.g. by protein kinase activators such as TPA) releases 6fold the amount of reactive oxygen species than do unprimed phagocytes. The ability of phagocytes to generate an

### A) Solvent Control

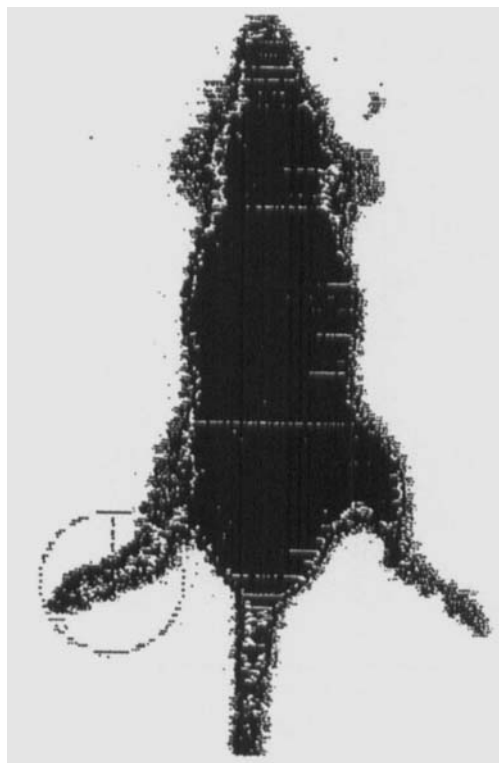
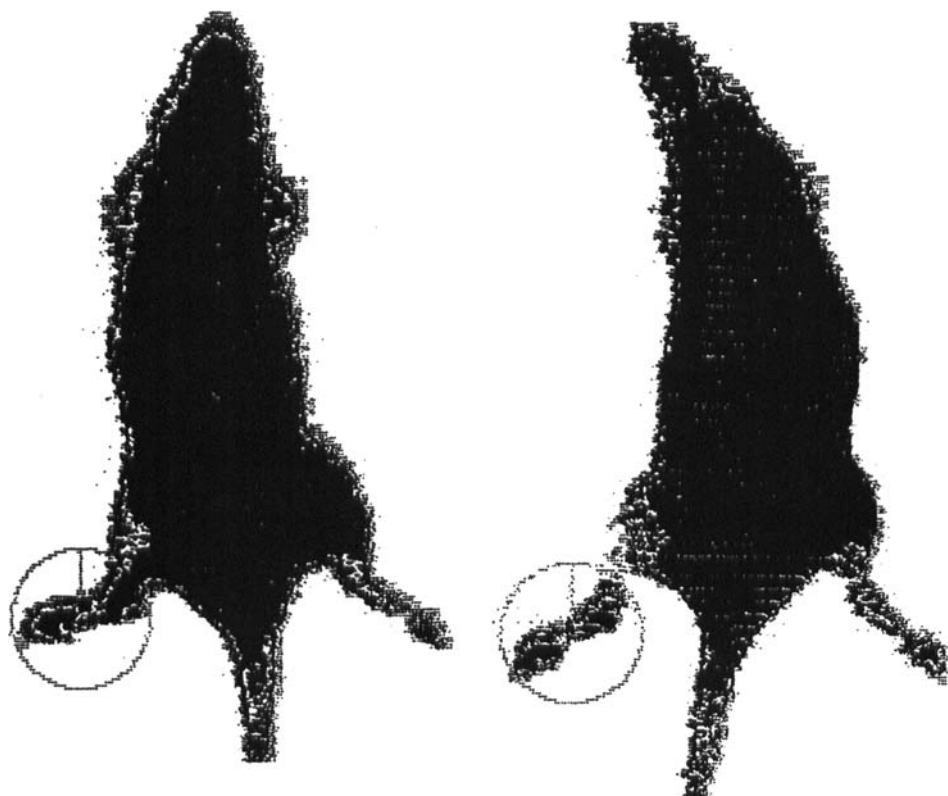


FIGURE 4  $^{99m}\text{Pertechnetate}$ -imaging and  $\text{K}_2\text{CrO}_8$ -arthritis in male Wistar rats. A) Solvent Control (48 hours after injection).

**B) 48 hours after  
arthritis induction**

**C) Day 12: Development of  
arthritis in non-injected  
(right) paw**



**FIGURE 4 continued** B) 48 hours after the intraplantar injection of  $3 \mu\text{mol/kg}$   $\text{K}_3\text{CrO}_8$  into the left hindpaw (maximal acute inflammatory response); C) development of arthritis in non-injected (right) paw 12 days after  $\text{K}_3\text{CrO}_8$ -treatment (maximal secondary response). The presented  $\gamma$ -scintigraphic scans of individual rats were typical for the status of arthritis in a group of ten. For experimental details see *Materials and Methods*.

oxidative burst is under cytokine control.<sup>23</sup> While pro-inflammatory cytokines including  $\text{TNF-}\alpha$ , IL-1 and IL-3, but also GM-CSF and  $\text{IFN-}\gamma$  are powerful enhancers of NADPH oxidase activity, its ROS production is down-regulated by anti-inflammatory cytokines like  $\text{TGF-}\beta$  and IL-4.  $\text{TNF-}\alpha$  has come to the fore as pivotal agent in this interactive cytokine network and plays a crucial role in the etiopathogenesis of rheumatic diseases.<sup>24</sup> The significance of  $\text{TNF-}\alpha$  in the development and maintenance of arthritis is evidenced by transgenic mice overexpressing this cytokine.<sup>25</sup> These mice develop arthritis at about 4 weeks of age, which can be totally abrogated by injection of a monoclonal anti- $\text{TNF-}\alpha$  antibody. The binding of  $\text{TNF-}\alpha$  to its receptor on phagocytes initiates various intracellular pathways including major cellular kinases like protein kinase C (PKC), protein kinase A (PKA), a serine protein kinase and phospholipase  $\text{A}_2$ .<sup>26</sup> At the same time,  $\text{TNF-}\alpha$  and  $\text{IFN-}\gamma$  induce the expression of genes

encoding for the gp91-*phox* and p47-*phox* subunits of the NADPH oxidase system.<sup>27</sup> The PKC-dependent phosphorylation of the p47 subunit modulates the priming state of phagocytes and initiates the assembly process of NADPH oxidase to the active enzyme.<sup>28</sup> The amount of priming of NADPH oxidase can be sensitively quantified by TPA-stimulated chemiluminescence. Whole blood CL is here used as immunosensor of inflammatory arthritis.

Recently, we demonstrated the collapse of the sulfhydryl-dependent antioxidant and antioxidase system in rheumatic patients.<sup>9</sup> In the absence of sufficient antioxidant protection the cytosolic transcription factor NF- $\kappa$ B gets activated by oxidative attack on its inhibiting subunit I- $\kappa$ B.<sup>29</sup> NF- $\kappa$ B travels then into the nucleus, where it mediates the expression of TNF- $\alpha$ , which in turn enhances the phagocytic production of ROS.<sup>30</sup> ROS-dependent oxidation of intracellular sulfhydryls are also intrinsically linked to the proliferation of lymphocytes.<sup>31</sup> This suggests that a stable loop forms between phagocytic ROS production, NF- $\kappa$ B-activation and cytokine expression, which links unspecific defenses of phagocytes to the activities of T and B cells. Imbalances in the pro- and anti-oxidant levels caused by acquired or induced dysfunctions of phagocytes in rheumatic diseases may cause chronic inflammation and eventually convert the disease to autoimmunization, most likely by the breakdown of self-tolerance. To test the hypothesis of ROS-induced arthritis, we used the simple, overlookable model of K<sub>3</sub>CrO<sub>8</sub> arthritis. The central chromium(V) atom in K<sub>3</sub>CrO<sub>8</sub> is tetrahedrally surrounded by four equivalent O<sub>2</sub><sup>2-</sup> groupings, while the binding length of chromium to oxygen differs by 0.096 Å (1.848 Å and 1.944 Å, respectively).<sup>12</sup> This causes an intramolecular tension. During the aqueous decay at physiological pH the Cr(V)-bound oxygen is released as superoxide, hydroxyl radicals, singlet oxygen and hydrogen peroxide, the same reactants which are produced by activated neutrophils and monocytes. ROS, derived from decaying K<sub>3</sub>CrO<sub>8</sub> degrade rapidly biopolymers including hyaluronic acid and collagen, cause lipid peroxidation, deplete the sulfhydryl-dependent antioxidant system in plasma and attract phagocytes to the primary inflammatory lesion.<sup>10</sup> Our study demonstrates that a single pulse of ROS, derived from the intraplantar application of micromolar concentrations of K<sub>3</sub>CrO<sub>8</sub> suffices to induce a long-lasting, self-perpetuating inflammatory process in mice and rats. Unlike most other models of chronic inflammation and arthritis the K<sub>3</sub>CrO<sub>8</sub>-induced arthritis represents a simple, reliable model with clearly defined reactants.

However, we can not exclude that Cr(VI)O<sub>4</sub><sup>2-</sup> formed during the aqueous decay of Cr(V)O<sub>8</sub><sup>3-</sup> participates in the inflammatory process. Chromate is well known to cause chromosome aberrations, mutations and transformations.<sup>32</sup> Cr(VI) causes DNA single strand breaks, alkali labile sites as well as DNA-protein crosslinks and renal damage, phenomena which are also observed in patients suffering from systemic lupus erythematosus and in congenital arthritis in MRL/lpr mice.<sup>33,34</sup> In addition, protein-protein crosslinking occurs and is the major principle of chromate tanning of leather, where neighbouring collagen fibers are bridged by chromium(III) bound to the carboxyl groups of the chain.<sup>35</sup> More importantly, chromate is a powerful and selective inhibitor of glutathione reductase, an ubiquitous enzyme responsible for keeping the intracellular GSH pools in a reduced state.<sup>36</sup> The inhibition of this enzyme by chromate causes the breakdown of the intracellular antioxidant barrier, which is a necessary prerequisite for proliferating lymphocytes.<sup>31</sup> In addition, the fall of GSH/GSSG ratios induced by chromate-inhibition of GSH reductase causes the subsequent inhibition of glutathione peroxidase, a further antioxidase involved in the decontamination of intracellular hydrogen peroxide.<sup>37</sup> Moreover, elevated levels of H<sub>2</sub>O<sub>2</sub> inactivate superoxide dismutase and catalase.<sup>37</sup> Subsequently, the breakdown of protection by major antioxidases and the

collapse of the GSH system causes the activation of NF- $\kappa$ B and the expression of pro-inflammatory cytokines, which prime phagocytic NADPH oxidases to the enhanced production of ROS.<sup>29</sup> Chromate toxicity has also been linked to the generation of hydroxyl radicals.<sup>38</sup> Cr(VI), which is easily taken up by cells can be reduced to Cr(V) by ascorbate and GSH, but also by the microsomal cytochrome P450 system.<sup>36,39</sup> The  $K_m$  for the microsomal reduction is 1.04  $\mu$ M and the reaction proceeds with  $v_{max}$  of 5.03 nmol/min/mg protein.<sup>40</sup> Similar to the Fe(II)/Fe(III)-driven Fenton reaction, Cr(V) catalyzes  $\cdot$ OH radical production in the presence of  $H_2O_2$ . This suggests that the aqueous decay of  $K_2CrO_8$  to ROS and chromate initiates a cascade of events, which eventually drives the acute inflammatory response (initially induced by ROS- injury and concomitant attraction of phagocytes into the inflammatory lesion) into a chronic process by chromate-dependent inhibition of major antioxidantases and breakdown of the sulfhydryl-dependent antioxidant system. At the same time, the ascorbate-, GSH-and/or cytochrome P450-dependent redox-cycling of Cr(VI)/Cr(V) forms a stable loop, which further enhances the intracellular stress by generating hydroxyl radicals. Further work is ongoing in our laboratory to investigate the arthritic reactivity of chromate in mice chronically exposed to this metal. Considering the ubiquitous environmental presence of chromium compounds and their widespread industrial use, further research seems warranted that thoroughly addresses the multitude of biochemical events that modulate chromium-dependent inflammation, arthritis and autoimmunity.

### Acknowledgments

We thank Professor Nicholas Avrion Mitchison, Berlin, for helpful discussions. The expert technical help of Regina Graetz, Berlin, Carola Spinnler, Regensburg, and Dorota Sanocka, Poznan, is gratefully appreciated.

### References

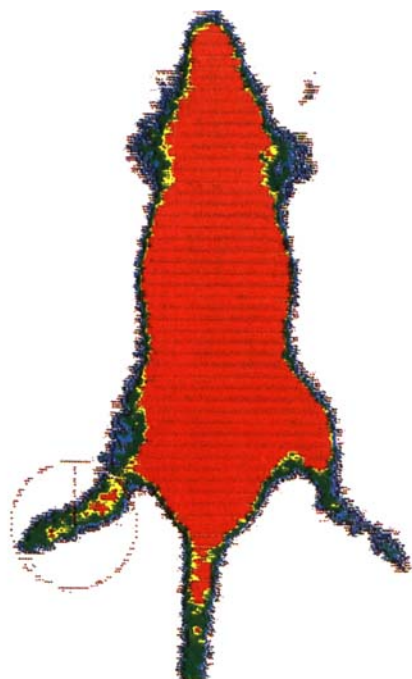
1. E.H. Yelin and W.R. Felts (1990) A summary of the impact of musculoskeletal conditions in the United States. *Arthritis and Rheumatism*, **33**, 750–755.
2. R. Holmdahl, M. Andersson, T.J. Goldschmidt, K. Gustafsson, L. Jansson and J.A. Mo (1990) Type II collagen autoimmunity in animals and provocations leading to arthritis. *Immunological Reviews*, **118**, 193–232.
3. P.H. Wooley, H.S. Luthra, J.M. Stuart and C.S. David (1981) Type II collagen-induced arthritis in mice. Major histocompatibility complex (I region) linkage and antibody response. *Journal of Experimental Medicine*, **154**, 688–700.
4. A.J. Lewis, R.P. Carlson and J. Chang (1985) Experimental models of inflammation. In *Handbook of inflammation 5: The pharmacology of inflammation* (eds. L.E. Glynn, J.C. Houk, G. Weissmann), Elsevier, Amsterdam, pp. 371–397.
5. J.M. Stuart, A.S. Townes and A.H. Kang (1982) The role of collagen autoimmunity in animal models and human diseases. *Journal of Investigational Dermatology*, **79**, 121–125.
6. K. Morgan, R.B. Clague, M.J. Shaw, S.A. Firth, T.M. Twose and P.J.L. Holt (1981) Native type II collagen-induced arthritis in the rat. The effect of complement depletion by a cobra venom factor. *Arthritis and Rheumatism*, **24**, 1356–1362.
7. T.W.J. Huizinga, D. Roos and A.E.G. von dem Borne (1990) Neutrophil Fc-gamma receptors: a two way bridge in the immune system. *Blood*, **75**, 1211–1214.
8. R. Miesel, H. Kröger, M. Zuber, R. Grätz, J. Neth (1994) Elevated levels of oxygen- and nitrogen-centered radicals in patients with inflammatory and autoimmune rheumatic diseases. *Zeitschr. Rheumatol.*, **53**, 6 [Abstract].
9. R. Miesel and M. Zuber (1993) Copper-dependent antioxidant defenses in inflammatory and autoimmune rheumatic diseases. *Inflammation*, **17**, 283–294.
10. R. Miesel and R. Haas (1993) Reactivity of an active center analogue of  $Cu_2Zn_2$  superoxide dismutase in murine model of acute and chronic inflammation. *Inflammation*, **17**, 595–611.
11. R. Miesel, D. Sanocka, M. Kurpisz and H. Kröger (1994) Anti-arthritic reactivity of NADPH oxidase inhibitors. *Inflammation*, in press.

12. W. Paschen (1975) Der Kaliumperoxochromat Zerfall. In *Cu(II)-Komplexe in der Biochemie aktivierter Sauerstoff-Spezies*, PhD Thesis, Tübingen, Germany, pp. 91–97.
13. R. Miesel and U. Weser (1988) Reactivity of active centre analogues of  $\text{Cu}_2\text{Zn}_2$  superoxide dismutase during the aqueous decay of  $\text{K}_3\text{CrO}_8$ . *Inorganica Chimica Acta*, **160**, 119–121.
14. R. Miesel and U. Weser (1991) Chemiluminescence assays of  $\text{Cu}_2\text{Zn}_2$  superoxide dismutase mimicking Cu-complexes. *Free Radical Research Communications*, **12**, 253–258.
15. E.H. Riesenfeld, H.E. Wohlers and W.A. Kutsch (1905) Höhere Oxydationsprodukte des Chroms. *Chemische Berichte*, **38**, 1885–1898.
16. P.H. Wooley (1988) Collagen-induced arthritis in the mouse. *Methods in Enzymology*, **162**, 361–373.
17. D. Sanocka (1994) *Personal Communication*.
18. H. Gyllenhammar (1987) Lucigenin chemiluminescence in the assessment of neutrophil superoxide production. *Journal of Immunological Methods*, **97**, 209–213.
19. R.C. Allen (1982) Biochemiexcitation: chemiluminescence and the study of biological oxygenation reactions. In *Chemical and Biological Generation of Excited States* (eds. W. Adam and P. Cilento), Academic Press, New York, pp. 309–344.
20. R. Stocker and B. Frei (1991) Endogenous antioxidant defences in human plasma. In *Oxidative Stress. Oxidants and Antioxidants* (ed. H. Sies), Academic Press, London, pp. 213–245.
21. I.A. Cree (1992) Assays of human phagocyte function using microtitre plate luminometers. In *Bioluminescence and Chemiluminescence* (eds. P.A. Stanley PA and L.J. Krick), Wiley, New York, pp. 262–264.
22. B.M. Babior, R. Kuver and J.T. Curnutte (1988) Kinetics of activation of the respiratory burst oxidase in a fully soluble system from human neutrophils. *Journal of Biological Chemistry*, **263**, 1713–1718.
23. K.I. Arai (1990) Cytokines: coordinators of immune and inflammatory responses. *Annual Reviews of Biochemistry*, **59**, 783–836.
24. B. Beutler and A. Cerami (1989) The biology of cachectin/TNF a primary mediator of the host response. *Annual Reviews of Immunology*, **7**, 625–655.
25. L. Aloe, L. Probert, G. Kollias, I. Bracci-Laudier, M.G. Spillantini and R. Levi-Montalcini (1993) The synovium of transgenic mice expressing human tumor necrosis factor contains a high level of nerve growth factor. *Growth Factors*, **9**, 149–155.
26. W.M. Williams, M.R. Ehrenstein and D.A. Isenberg (1994) The background to autoimmunity. In *The Handbook of Immunopharmacology. Immunopharmacology of Joints and Connective Tissue* (eds. M.E. Davies and J.T. Dingle), Academic Press, London, pp. 1–34.
27. J.W. Gupta, M. Kubin, L. Hartman, M. Cassatella and G. Trinchieri (1992) Induction of expression of genes encoding components of the respiratory burst oxidase during differentiation of human myeloid cell lines induced by tumor necrosis factor and gamma-interferon. *Cancer Research*, **52**, 2530–2537.
28. D.R. Ambruso, B.G.J.M. Bolscher, P.M. Stokman, A.J. Verhoeven and D. Roos (1990) Assembly and activation of NADPH: $\text{O}_2$  oxidoreductase in human neutrophils after stimulation with phorbolmyristate acetate. *Journal of Biological Chemistry*, **265**, 924–930.
29. R. Schreck, K. Albermann and P. Baeuerle (1992) Nuclear factor  $\kappa\text{B}$ : an oxidative stress-responsive transcription factor of eukaryotic cells (a review). *Free Radical Research Communications*, **17**, 221–237.
30. M.J. Lenardo and D. Baltimore (1989) NF- $\kappa\text{B}$ : a pleiotropic mediator of inducible and tissue-specific gene control. *Cell*, **58**, 227–229.
31. F.J.T. Staal, M. Roederer, L.A. Herzenberg and L.A. Herzenberg (1990) Intracellular thiols regulate activation of nuclear factor kappa B and transcription of human immunodeficiency virus. *Proceedings of the National Academy of Sciences USA*, **87**, 9943–9947.
32. M. Sugiyama, K. Tsuzuki and R. Ogura (1991) Effect of ascorbic acid on DNA damage, cytotoxicity, glutathione reductase, and formation of paramagnetic chromium in chinese hamster V-79 cells treated with sodium chromate(VI). *Journal of Biological Chemistry*, **266**, 3383–3386.
33. C.A. Miller, M.D. Cohen and M. Costa (1991) Complexing of actin and other nuclear proteins to DNA by cis-diaminedichloroplatinum (II) and chromium compounds. *Carcinogenesis*, **12**, 269–276.
34. B.S. Andrews, R.A. Eisenberg, A.N. Theofilopoulos, S. Izui, C.B. Wilson, P.J. McConahey, M.D. Murphy, J.B. Roths and F.J. Dixon (1978) Spontaneous murine-like syndromes. Clinical and immunopathological manifestations in several strains. *Journal of Experimental Medicine*, **148**, 1198–1204.
35. J. Gustavson (1956) The chemistry of tanning processes. Academic Press, New York, pp. 44–56.
36. M. Sugiyama, K. Tsuzuki and N. Haramki (1993) Influence of o-phenanthroline on DNA single-strand breaks, alkali-labile sites, glutathione reductase, and formation of chromium(V) in Chinese hamster V-79 cells and treated with sodium chromate(VI). *Archives of Biochemistry and Biophysics*, **305**, 261–266.
37. B. Halliwell and J.M.C. Gutteridge (1989) Protection against oxidants in biological systems: the superoxide theory of oxygen toxicity. In *Free radicals in biology and medicine* (eds. B. Halliwell B and J.M.C. Gutteridge), Clarendon Press, Oxford, pp. 86–187.

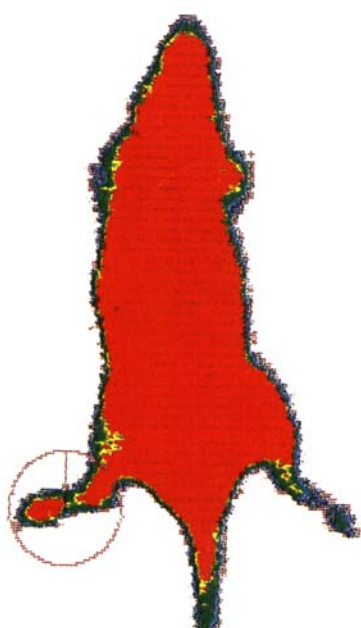


38. H.H. Poer and A. Woldrich (1991) Oxygen radical formation, a probable mechanism for chromate toxicity. *Progress in Histochemistry and Cytochemistry*, **23**, 220–226.
39. A. Mikalsen, J. Alexander and R.A. Andersen (1991) Effect of in vivo chromate, acetone and combined treatment on rat liver in vitro microsomal chromium(VI) reductive activity and on cytochrome P450 expression. *Pharmacology and Toxicology* **68**, 456–463.
40. P.F. Pratt and C.R. Myers (1993) Enzymatic reduction of chromium(VI) by human hepatic microsomes. *Carcinogenesis*, **14**, 2051–2057.

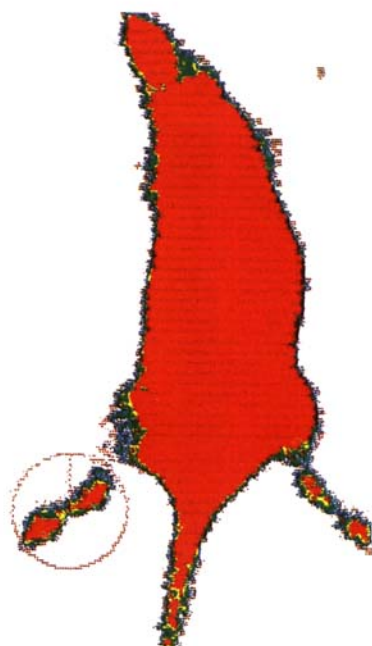
Accepted by Professor H. Sies



A) Solvent Control



B) 48 hours after arthritis induction



C) Day 12: Development of arthritis in non-injected (right) paw

FIGURE 4  $\text{Na}^{99\text{m}}\text{TcO}_4$ -Imaging of male Wistar Rats suffering from  $\text{K}_2\text{CrO}_8$ -Arthritis.